

Supplementary Material

A theoretical model on the formation mechanism and kinetics of highly toxic air pollutants from halogenated formaldehydes reacted with halogen atoms

Y.M. Ji¹, H.H. Wang^{1,2}, Y.P. Gao^{1,2}, G.Y. Li¹, and T.C. An^{1,*}

[1] State Key Laboratory of Organic Geochemistry and Guangdong Key Laboratory of Environmental Resources Utilization and Protection, Guangzhou Institute of Geochemistry, Chinese Academy of Sciences, Guangzhou 510640, China;
[2] Graduate School of Chinese Academy of Sciences, Beijing 100049, China.

Correspondence to: T.C. An (antc99@gig.ac.cn)

■ METHODS

Selection of Methods. In this work, at least 40 pathways have been calculated for the title reactions. Although the calculated time of energies for every stationary point needed for high-accuracy methods were not too long, the cumulative time for all of these stationary points were huge and not neglectable. Thus, the developments of a suitable method to balance the relationship between the computational accuracy and the computational expensive were very necessary.

In this study, the results obtained at the quadratic configuration interaction with single, double and triple excitations [QCISD(T)] methods were selected from the reference (Wu et al., 2003) (Table S1). The QCISD(T) method, a costly single-point energy (SPE) calculation method coupled with a large basis set [6-311+G(3df,2p)], could effectively minimize the error from the correlation of electrons and spin contamination effect in SPE calculation (Szabo et al., 1997). The computational results indicated that the values of PMP2//MP2 level are more closer to the values of QCISD(T) level than those of MP2//MP2 level, within the error limit of 0.47 kcal/mol. Thus, to meet the need of both high accuracy and low computational cost, the

PMP2//MP2 level was selected to carry out the calculation of the mechanisms and kinetics.

■ RESULTS AND DISCUSSION

Energies. For the pathways of F-R_{abs-Cl}, Cl-R_{abs-Cl}, F-R_{abs-Br}, Cl-R_{abs-Br} and Br-R_{abs-Br}, the energy barrier heights were obtained respectively as 1.88, 1.83, 1.34, 0.94 and 3.24 kcal/mol without the ZPE corrections, but the data become negative via the ZPE correction. For testifying the negative energy barrier height, the formula $E_{a,298} = \Delta E_T^\ddagger + RT$ was used as a simple estimation of the activation energy (Pacey, 1981), where $\Delta E_T^\ddagger = V_B + \Delta ZPE + \Delta E(T)$, V_B and $E(T)$ represent the energy barrier height and thermal energy correction. The estimated activation energies of the pathways of F-R_{abs-Cl}, Cl-R_{abs-Cl}, F-R_{abs-Br}, Cl-R_{abs-Br} and Br-R_{abs-Br} were -2.92, -4.72, -2.78, -4.00 and -4.01 kcal/mol, respectively, which implied that all the aforementioned pathways could be nearly barrierless (Ji et al., 2008).

Rate Constants. The canonical variational transition state theory (CVT) (Truhlar et al., 1980) rate constant can be obtained by variationally minimizing the generalized transition-state theory rate constant $k^{GT}(T,s)$ with respect to the dividing surface at s , that is,

$$k^{CVT}(T) = \min_s k^{GT}(T,s) \quad (1)$$

where

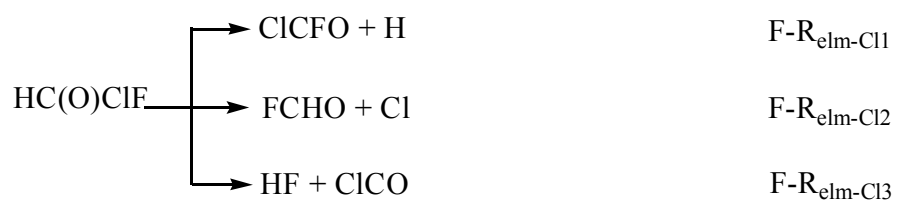
$$k^{GT}(T,s) = \frac{\sigma}{h\beta} \frac{Q^{GT}(t,s)}{Q^R(T)} \exp[-\beta V_{MEP}(s)] \quad (2)$$

In these equations, s is the location of the generalized transition state on the intrinsic reaction coordinate (IRC); σ is the symmetry factor accounting for the possibility of two or more symmetry-related reaction paths; β equals $(k_B T)^{-1}$ where k_B is Boltzmann's constant, h is Planck's constant; $Q^R(T)$ is the reactant's partition function per unit volume, excluding symmetry numbers for rotation; $V_{MEP}(s)$ is the classical energy along the minimum-energy path (MEP) overall zero of energy at the reactants; $Q^{GT}(T,s)$ is the partition function of generalized transition state at s with the local zero of energy at $V_{MEP}(s)$ and with all rotational symmetry numbers set to unity. To include the tunneling effect, the CVT rate constant is multiplied by a transmission coefficient computed with the small-curvature tunneling (SCT) (Liu et al., 1993) approximation, which is denoted by $k(CVT/SCT)$. The total rate constants for the title reactions are obtained from the sum of the individual rate constants associated.

Branching Ratio. The branching ratio Γ of each pathways was determined on the following equation, $\Gamma_n = \frac{k_n}{\sum_n k_n}$, where k_n is the reaction rate constants of n th pathway. In this work, the

total CVT/SCT rate constants for each atmospheric reaction were obtained as the sum of the individual rate constants associated with the H-abstraction and X-addition pathways.

The Atmospheric Fate of ClCO Radical. To confirm the no barrier of these processes, the point-wise potential curve was calculated and the results is shown in [Figure S7-S9](#). For the pathways 2 and 3, the forming C–O bonds were fixed at the values from 1.1 to 2.7 Å and from 1.2 to 3.2 Å with the interval of 0.1 Å, respectively, and the other geometric parameters were optimized for each C–O value. The minimum energy in these two pathways appeared at the C–O distance of 1.4 Å, leading to intermediates *tran*-ClCO₃ and *cis*-ClCO₃, respectively. As for the pathway 4, the forming C–Cl bond was fixed at the values from 1.3 to 4.5 Å with the interval of 0.1 Å, and the other geometric parameters were optimized for each C–Cl value. The minimum energy appeared at the C–Cl distance of 1.8 Å, leading to phosgene.



Scheme S1. For the addition intermediate HC(O)ClF , three degradation pathways: H-elimination, Cl-elimination, and HF-elimination pathways

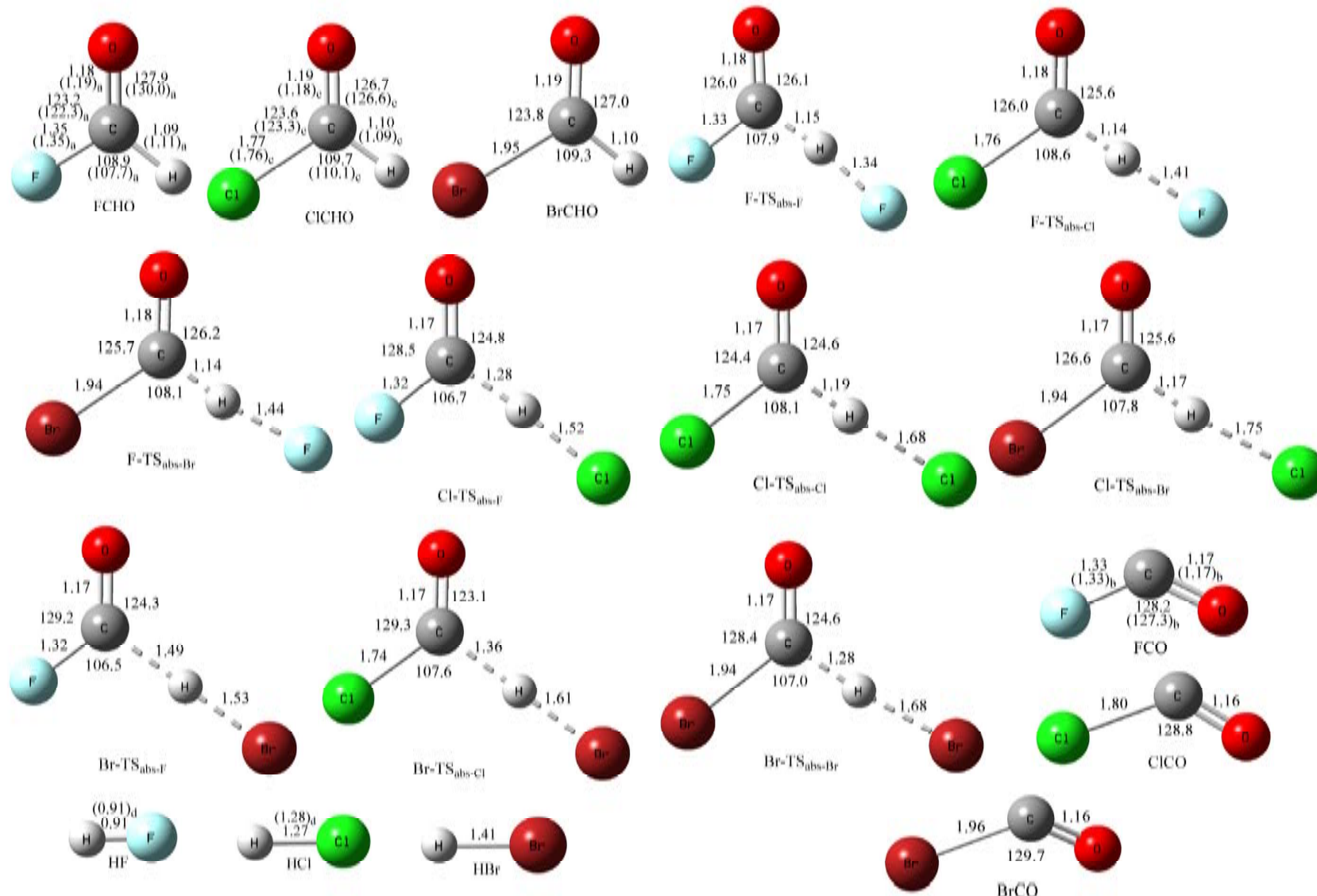


Figure S1. Optimized geometries of reactants, transition states and products involved in the H-abstraction pathways at the MP2/6-311G(d,p) level as well as the available experimental data. (Groner et al., 2001; Huisman et al., 1979; Nagai et al., 1981; NIST). (Bond lengths are in Å and angles are in °.)

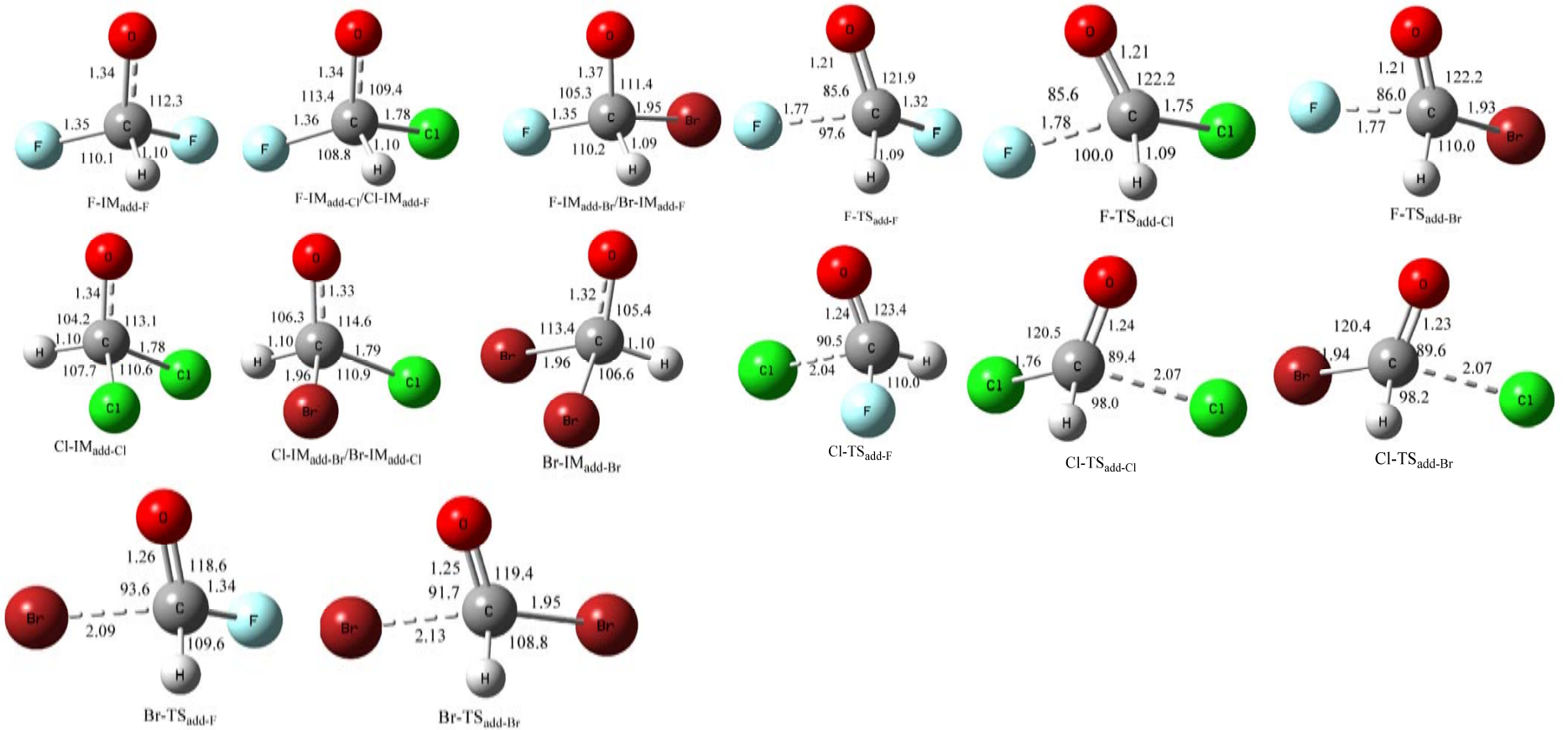


Figure S2. Optimized geometries of reactants, transition states, intermediates and products involved in the X-addition pathways at the MP2/6-311G(d,p) level. (Bond lengths are in Å and angles are in °.)

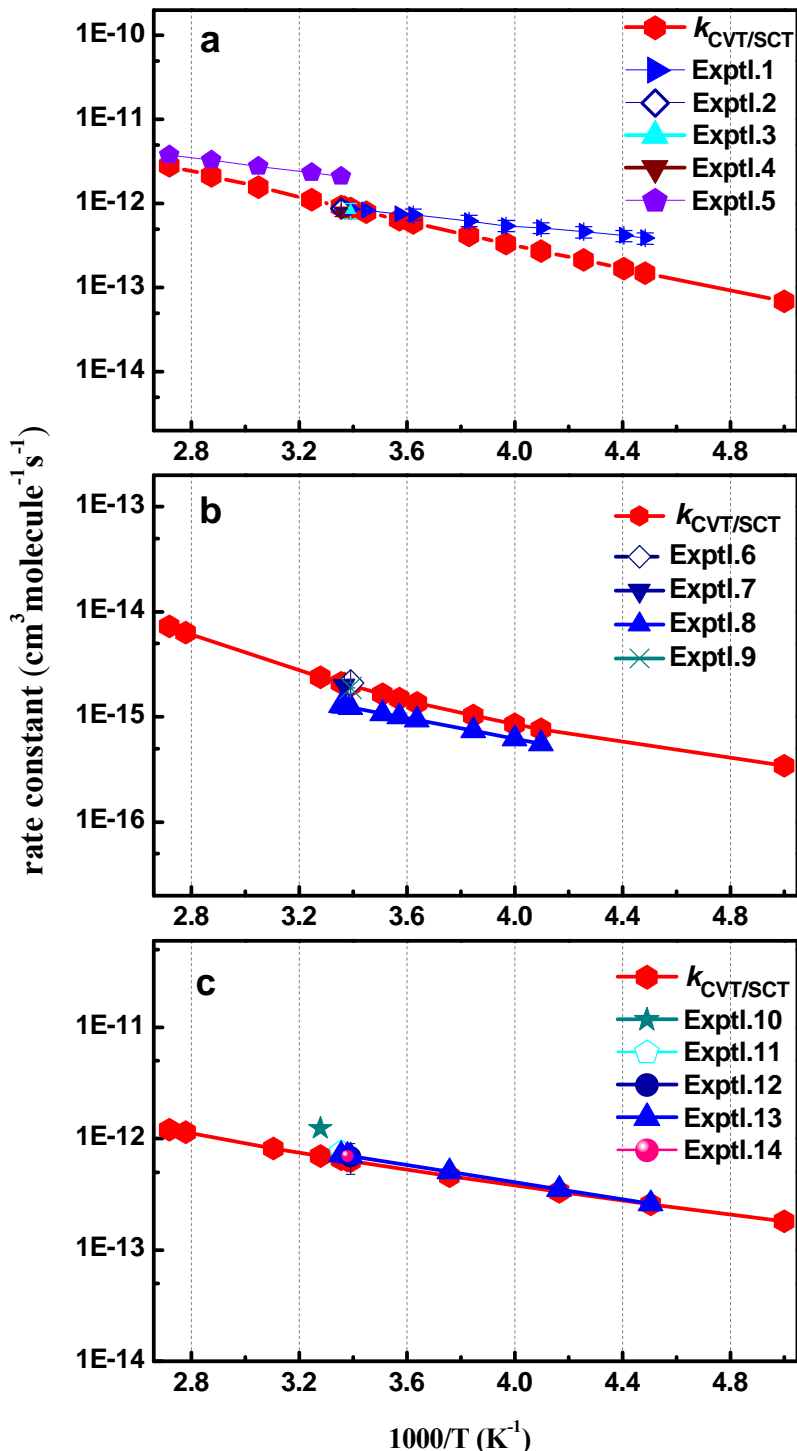


Fig. S3. Plot of the CVT/SCT rate constants calculated at the PMP2//MP2 level and the available experimental values vs $1000/T$ between 200–368 K for the H-abstraction pathways of (a) FCHO with F, (b) FCHO with Cl, and (c) ClCHO with Cl. Exptl. 1 from (Behr et al., 1998); Exptl. 2 from (Behr et al., 1993); Exptl. 3 from (Meagher et al., 1997); Exptl. 4 from (Hasson et al., 1998); Exptl. 5 from (Francisco et al., 1990); Exptl. 6 from (Edney et al., 1992); Exptl. 7 from (Wallington et al., 1992); Exptl. 8 from (Bednarek et al., 1996); Exptl. 9 from (Meagher et al., 1997); Exptl. 10 from (Sanhueza et al., 1975); Exptl. 11 from (Libuda et al., 1990); Exptl. 12 from (Wallington et al., 1996); Exptl. 13 from (Orlando, 1999); Exptl. 14 from (Catoire et al., 1996).

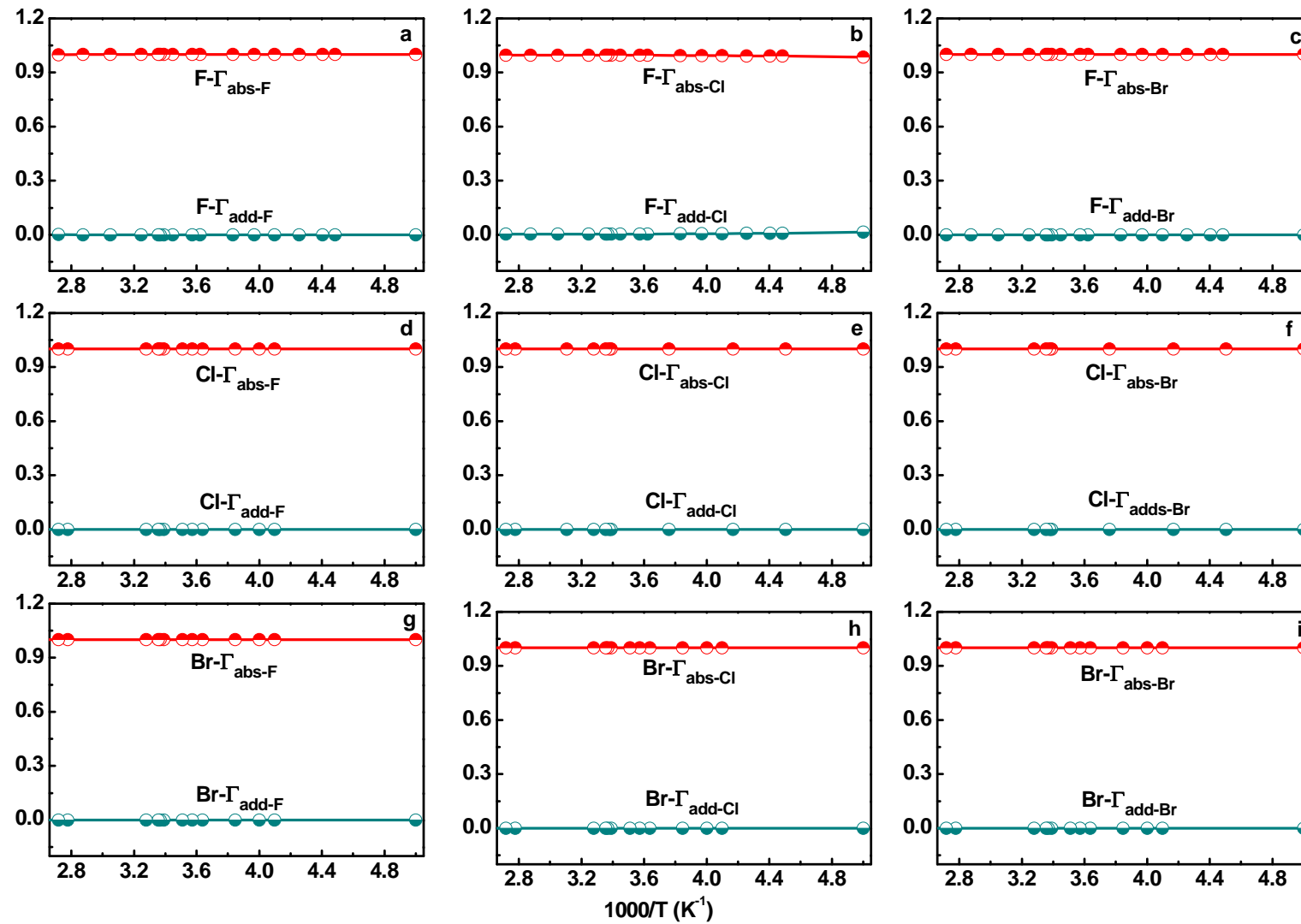


Figure S4. Plot of calculated branching ratio of the H-abstraction and X-addition pathways versus $1000/T$ between 200 and 368 K for the reactions of (a) FCHO with F, (b) ClCHO with F, (c) BrCHO with F, (d) FCHO with Cl, (e) ClCHO with Cl, (f) BrCHO with Cl, (g) FCHO with Br, (h) ClCHO with Br and (i) BrCHO with Br.

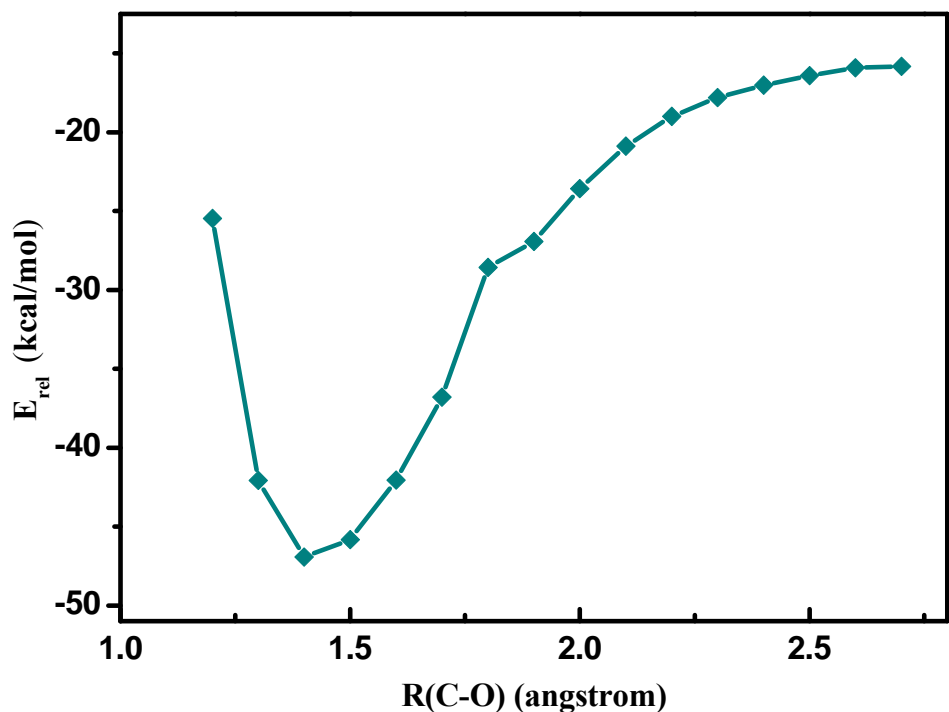


Figure S5. Potential energy curve for the formative process of *trans*-CClO₃ at the MP2/6-311G(d,p) level. The dotted line denotes the relative energy of ClCO + O₂.

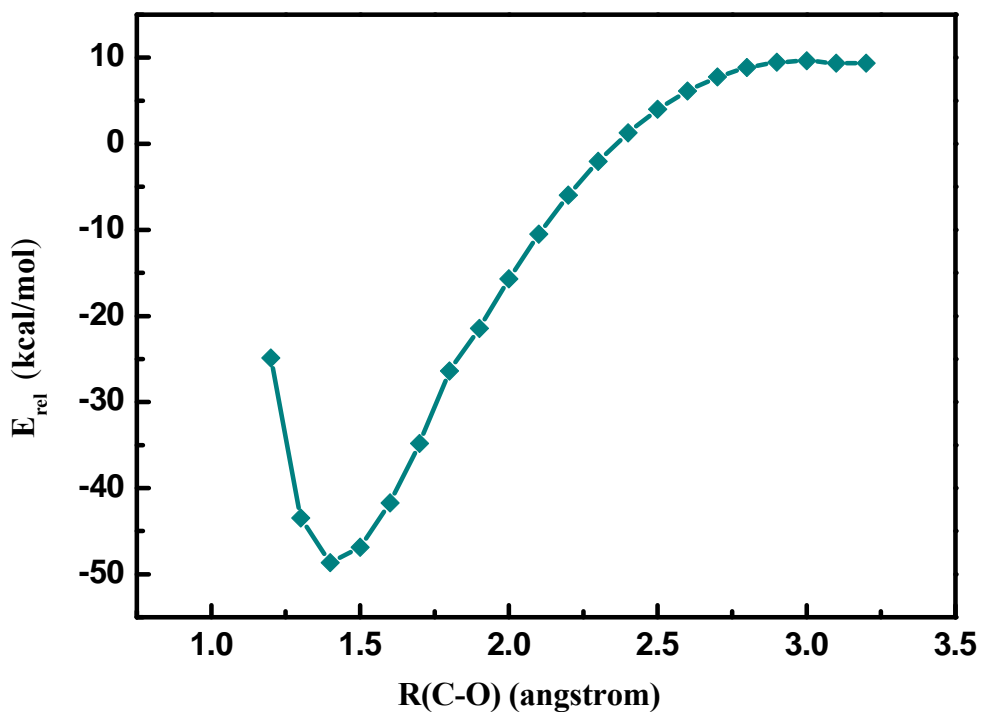


Figure S6. Potential energy curve for the formative process of *cis*-CClO₃ at the MP2/6-311G(d,p) level. The dotted line denotes the relative energy of ClCO + O₂.

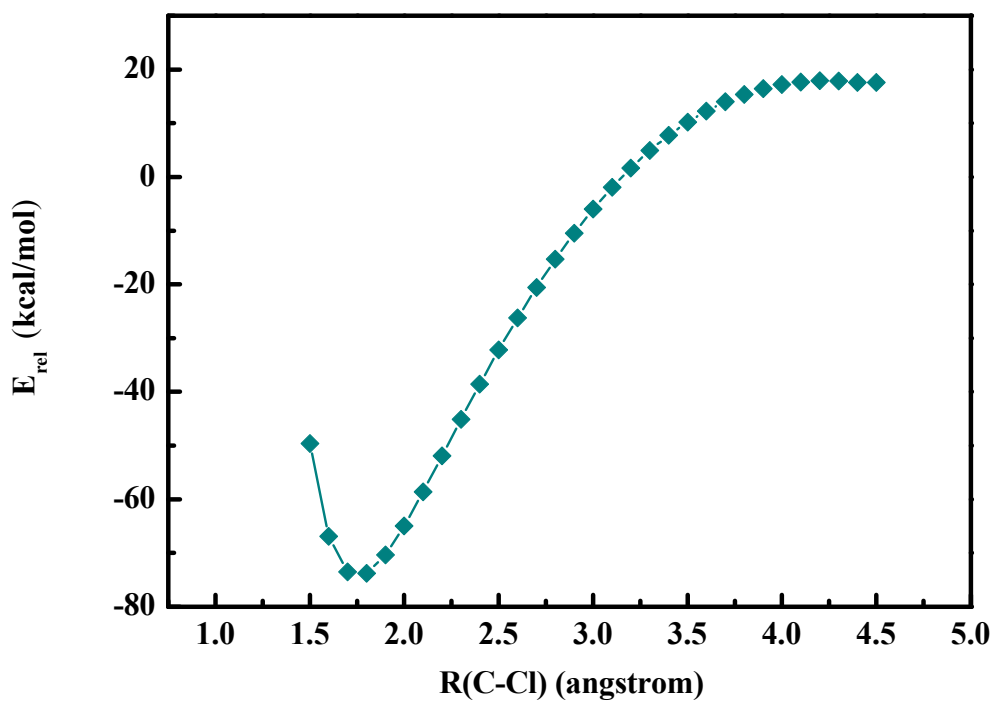


Figure S7. Potential energy curve for the formative process of phosgene at the MP2/6-311G(d,p) level. The dotted line denotes the relative energy of $\text{ClCO} + \text{Cl}$.

Table S1. The potential energies (ΔE) of the selected reaction pathways at the various levels. (in kcal/mol)

	^c MP2//MP2	^d PMP2//MP2	^e QCISD(T)//MP2	^f QCISD(T)//MP4	^g MP4//MP2
^a F-R _{abs-F}	3.06	1.29	1.76	1.51	2.9
^b F-R _{add-F}	15.37	6.20	5.1	5.8	6.4

^a The H-abstraction of the reaction of FCHO with F atom;

^b The X-addition of the reaction of FCHO with F atom;

^c The values at the MP2/6-311+G(3df,3pd)//MP2/6-311G(d,p) calculated by this work;

^d The values at the PMP2/6-311+G(3df,3pd)//MP2/6-311G(d,p) calculated by this work;

^e The values at the QCISD(T)/6-311+G(3df,2p)//MP2/6-311+G(d,p) calculated by Wu et al.;([Wu et al., 2003](#))

^f The values at the QCISD(T)/6-311+G(3df,2p)//MP4SDQ/6-311+G(d,p) calculated by Wu et al.;([Wu et al., 2003](#))

^g The values at the MP4SDQ/6-311+G(d,p)//MP2/6-311G(d,p) calculated by Francisco et al. ([Francisco et al., 1990](#))

Table S2. Calculated frequencies of the stationary points at the MP2/6-311G(d,p) level.

species	v	species	v
FCHO	672, 1056, 1097, 1413, 1882, 3158	ClCHO	468, 757, 967, 1387, 1812, 3115
BrCHO	365, 656, 927, 1344, 1814, 3101	FCO	643, 1081, 1995
ClCO	375, 631, 1973	BrCO	289, 569, 1945
HF	4252	HCl	3088
HBr	2741	FCCIO	421, 510, 678, 773, 1116, 1923
F ₂ CO	590, 626, 788, 976, 1265, 1998	FCBrO	352, 397, 635, 731, 1093, 1916
F-IM _{add-F}	478, 521, 656, 1007, 1153, 1176, 1362, 1414, 3093	F-IM _{add-Cl} /Cl-IM _{add-F}	257, 405, 589, 761, 1044, 1122, 1244, 1357, 3107
F-IM _{add-Br} /Br-IM _{add-F}	212, 310, 590, 600, 1030, 1137, 1171, 1389, 3141	Cl-IM _{add-Cl}	295, 337, 450, 695, 801, 1077, 1215, 1268, 3067
Cl-IM _{add-Br} /Br-IM _{add-Cl}	168, 235, 434, 592, 763, 1052, 1113, 1255, 3077	Br-IM _{add-Br}	174, 253, 361, 572, 683, 1078, 1099, 1208, 3057
F-TS _{abs-F}	1446 <i>i</i> , 83, 95, 625, 861, 985, 1126, 1343, 1972	F-TS _{abs-Cl}	886 <i>i</i> , 66, 88, 462, 731, 922, 1231, 1306, 1980
F-TS _{abs-Br}	732 <i>i</i> , 56, 82, 365, 587, 881, 1190, 1527, 1955	Cl-TS _{abs-F}	1552 <i>i</i> , 114, 231, 331, 704, 951, 1115, 1148, 2037
Cl-TS _{abs-Cl}	903 <i>i</i> , 81, 194, 443, 607, 813, 935, 1246, 2035	Cl-TS _{abs-Br}	481 <i>i</i> , 61, 171, 368, 589, 899, 1087, 1305, 1984
Br-TS _{abs-F}	805 <i>i</i> , 98, 199, 411, 744, 769, 885, 1118, 2025	Br-TS _{abs-Cl}	1210 <i>i</i> , 89, 222, 248, 500, 752, 861, 1045, 2071
Br-TS _{abs-Br}	1319 <i>i</i> , 68, 211, 229, 376, 683, 863, 1104, 2039	F-TS _{add-F}	1199 <i>i</i> , 301, 422, 688, 1071, 1165, 1425, 1641, 3202
F-TS _{add-Cl} /Cl-TS _{elm-F2}	1192 <i>i</i> , 247, 397, 488, 800, 1033, 1404, 1567, 3162	F-TS _{add-Br} /Br-TS _{elm-F2}	1206 <i>i</i> , 210, 359, 415, 688, 1022, 1362, 1561, 3144
Cl-TS _{add-F} /F-TS _{elm-Cl2}	899 <i>i</i> , 282, 357, 655, 955, 1144, 1370, 1463, 3176	Cl-TS _{add-Cl}	888 <i>i</i> , 223, 338, 467, 764, 964, 1366, 1388, 3149
Cl-TS _{add-Br} /Br-TS _{elm-Cl2}	893 <i>i</i> , 179, 328, 371, 658, 958, 1331, 1376., 3133	Br-TS _{add-F} /F-TS _{elm-Br2}	605 <i>i</i> , 275, 305, 633, 907, 1130, 1311, 1423, 3158
Br-TS _{add-Cl} /Cl-TS _{elm-Br2}	702 <i>i</i> , 202, 290, 455, 737, 932, 1314, 1366, 3141	Br-TS _{add-Br}	714 <i>i</i> , 150, 287, 358, 639, 921, 1308, 1326, 3128
F-TS _{elm-F1}	1776 <i>i</i> , 558, 562, 778, 836, 860, 1063, 1203, 1861	F-TS _{elm-Cl1} /Cl-TS _{elm-F1}	1773 <i>i</i> , 393, 445, 635, 696, 770, 852, 1072, 1873
F-TS _{elm-Br1} /Br-TS _{elm-F1}	1396 <i>i</i> , 312, 359, 628, 707, 739, 821, 1054, 2281	Cl-TS _{elm-Cl1}	1776 <i>i</i> , 292, 404, 501, 601, 607, 730, 792, 1888
Cl-TS _{elm-Br1} /Br-TS _{elm-Cl1}	1464 <i>i</i> , 228, 331, 509, 566, 660, 712, 772, 2341	F-TS _{elm-F3}	702 <i>i</i> , 394, 572, 718, 933, 1124, 1198, 1833, 2184
F-TS _{elm-Br3}	672 <i>i</i> , 255, 346, 575, 644, 760, 1173, 1824, 2408	F-TS _{elm-Cl3}	630 <i>i</i> , 324, 453, 619, 756, 859, 1176, 1734, 2339

Table S3. The imaginary frequencies and parameter L at the MP2 level. (ν in cm^{-1})

	F		Cl		Br	
	ν	L	ν	L	ν	L
FCHO	$1446i$	0.14	$1552i$	0.72	$805i$	3.50
ClCHO	$886i$	0.10	$903i$	0.22	$1210i$	1.30
BrCHO	$732i$	0.09	$481i$	0.15	$1319i$	0.67

Table S4. The enthalpies of formation ($\Delta H_{f,298}^0$) of the main species at PMP2//MP2 level.
(in kcal/mol)

species	enthalpies	species	enthalpies
FCHO	-93.53 ^a (-89.96)	FCO	-42.95 ^a (-41.04)
ClCHO	-46.55	ClCO	-6.16
BrCHO	-33.46 ± 0.3	BrCO	1.78 ± 0.3

^a Experimental values.(NIST)

Table S5. Calculated CVT/SCT rate constants of H-abstraction and X-addition pathways of the F + QCHO reaction system. (in $\text{cm}^3 \text{ molecule}^{-1} \text{ s}^{-1}$)

T(K)	F + FCHO → products			F + ClCHO → products			F + BrCHO → products		
	F- $k_{\text{abs-F}}$	F- $k_{\text{add-F}}$	k_{total}	F- $k_{\text{abs-Cl}}$	F- $k_{\text{add-Cl}}$	k_{total}	F- $k_{\text{abs-Br}}$	F- $k_{\text{add-Br}}$	k_{total}
200	6.84×10^{-14}	2.83×10^{-19}	6.84×10^{-14}	1.82×10^{-13}	2.57×10^{-15}	1.85×10^{-13}	1.44×10^{-12}	2.41×10^{-21}	1.44×10^{-12}
223	1.49×10^{-13}	1.46×10^{-18}	1.49×10^{-13}	3.30×10^{-13}	2.98×10^{-15}	3.33×10^{-13}	2.10×10^{-12}	2.43×10^{-20}	2.10×10^{-12}
227	1.69×10^{-13}	1.93×10^{-18}	1.69×10^{-13}	3.63×10^{-13}	3.07×10^{-15}	3.66×10^{-13}	2.24×10^{-12}	3.57×10^{-20}	2.24×10^{-12}
235	2.13×10^{-13}	3.35×10^{-18}	2.13×10^{-13}	4.36×10^{-13}	3.25×10^{-15}	4.39×10^{-13}	2.54×10^{-12}	7.53×10^{-20}	2.54×10^{-12}
244	2.74×10^{-13}	6.07×10^{-18}	2.74×10^{-13}	5.29×10^{-13}	3.48×10^{-15}	5.32×10^{-13}	2.90×10^{-12}	1.66×10^{-19}	2.90×10^{-12}
252	3.37×10^{-13}	1.00×10^{-17}	3.37×10^{-13}	6.23×10^{-13}	3.70×10^{-15}	6.27×10^{-13}	3.24×10^{-12}	3.22×10^{-19}	3.24×10^{-12}
261	4.20×10^{-13}	1.72×10^{-17}	4.20×10^{-13}	7.42×10^{-13}	3.97×10^{-15}	7.46×10^{-13}	3.66×10^{-12}	6.47×10^{-19}	3.66×10^{-12}
276	5.91×10^{-13}	3.95×10^{-17}	5.91×10^{-13}	9.74×10^{-13}	4.50×10^{-15}	9.79×10^{-13}	4.41×10^{-12}	1.89×10^{-18}	4.41×10^{-12}
280	6.44×10^{-13}	4.87×10^{-17}	6.44×10^{-13}	1.04×10^{-12}	4.66×10^{-15}	1.04×10^{-12}	4.62×10^{-12}	2.47×10^{-18}	4.62×10^{-12}
290	7.92×10^{-13}	8.05×10^{-17}	7.92×10^{-13}	1.23×10^{-12}	5.08×10^{-15}	1.24×10^{-12}	5.18×10^{-12}	4.68×10^{-18}	5.18×10^{-12}
295	8.74×10^{-13}	1.02×10^{-16}	8.74×10^{-13}	1.33×10^{-12}	5.31×10^{-15}	1.34×10^{-12}	5.47×10^{-12}	6.35×10^{-18}	5.47×10^{-12}
297	9.08×10^{-13}	1.12×10^{-16}	9.08×10^{-13}	1.37×10^{-12}	5.41×10^{-15}	1.38×10^{-12}	5.58×10^{-12}	7.15×10^{-18}	5.58×10^{-12}
298	9.26×10^{-13}	1.18×10^{-16}	9.26×10^{-13}	1.39×10^{-12}	5.46×10^{-15}	1.40×10^{-12}	5.64×10^{-12}	7.59×10^{-18}	5.64×10^{-12}
308	1.11×10^{-12}	1.85×10^{-16}	1.11×10^{-12}	1.62×10^{-12}	5.97×10^{-15}	1.63×10^{-12}	6.26×10^{-12}	1.34×10^{-17}	6.26×10^{-12}
328	1.57×10^{-12}	4.22×10^{-16}	1.57×10^{-12}	2.13×10^{-12}	7.19×10^{-15}	2.14×10^{-12}	7.59×10^{-12}	3.80×10^{-17}	7.59×10^{-12}
348	2.14×10^{-12}	8.86×10^{-16}	2.14×10^{-12}	2.74×10^{-12}	8.70×10^{-15}	2.75×10^{-12}	9.05×10^{-12}	9.64×10^{-17}	9.05×10^{-12}
368	2.84×10^{-12}	1.73×10^{-15}	2.84×10^{-12}	3.45×10^{-12}	1.06×10^{-14}	3.46×10^{-12}	1.06×10^{-11}	2.22×10^{-16}	1.06×10^{-11}

Table S6. Calculated CVT/SCT rate constants of H-abstraction and X-addition pathways of the Cl + QCHO reaction system. (in $\text{cm}^3 \text{ molecule}^{-1} \text{ s}^{-1}$)

T(K)	Cl + FCHO → products			Cl + ClCHO → products			Cl + BrCHO → products		
	Cl- $k_{\text{abs-F}}$	Cl- $k_{\text{add-F}}$	k_{total}	Cl- $k_{\text{abs-Cl}}$	Cl- $k_{\text{add-Cl}}$	k_{total}	Cl- $k_{\text{abs-Br}}$	Cl- $k_{\text{add-Br}}$	k_{total}
200	3.46×10^{-16}	4.55×10^{-31}	3.46×10^{-16}	1.82×10^{-13}	3.86×10^{-38}	1.82×10^{-13}	7.58×10^{-13}	1.13×10^{-33}	7.58×10^{-13}
244	7.61×10^{-16}	7.62×10^{-28}	7.61×10^{-16}	3.51×10^{-13}	7.65×10^{-35}	3.51×10^{-13}	1.14×10^{-12}	6.62×10^{-30}	1.14×10^{-12}
250	8.50×10^{-16}	1.72×10^{-27}	8.50×10^{-16}	3.79×10^{-13}	1.79×10^{-34}	3.79×10^{-13}	1.20×10^{-12}	1.71×10^{-29}	1.20×10^{-12}
260	1.03×10^{-15}	6.14×10^{-27}	1.03×10^{-15}	4.29×10^{-13}	6.87×10^{-34}	4.29×10^{-13}	1.30×10^{-12}	7.55×10^{-29}	1.30×10^{-12}
275	1.36×10^{-15}	3.49×10^{-26}	1.36×10^{-15}	5.11×10^{-13}	4.50×10^{-33}	5.11×10^{-13}	1.46×10^{-12}	5.75×10^{-28}	1.46×10^{-12}
280	1.50×10^{-15}	5.99×10^{-26}	1.50×10^{-15}	5.40×10^{-13}	8.19×10^{-33}	5.40×10^{-13}	1.51×10^{-12}	1.08×10^{-27}	1.51×10^{-12}
285	1.65×10^{-15}	1.01×10^{-25}	1.65×10^{-15}	5.70×10^{-13}	1.47×10^{-32}	5.70×10^{-13}	1.56×10^{-12}	1.98×10^{-27}	1.56×10^{-12}
295	1.99×10^{-15}	2.71×10^{-25}	1.99×10^{-15}	6.33×10^{-13}	4.62×10^{-32}	6.33×10^{-13}	1.68×10^{-12}	6.27×10^{-27}	1.68×10^{-12}
297	2.07×10^{-15}	3.28×10^{-25}	2.07×10^{-15}	6.46×10^{-13}	5.78×10^{-32}	6.46×10^{-13}	1.70×10^{-12}	7.82×10^{-27}	1.70×10^{-12}
298	2.11×10^{-15}	3.60×10^{-25}	2.11×10^{-15}	6.52×10^{-13}	6.47×10^{-32}	6.52×10^{-13}	1.71×10^{-12}	8.73×10^{-27}	1.71×10^{-12}
305	2.40×10^{-15}	6.85×10^{-25}	2.40×10^{-15}	6.99×10^{-13}	1.41×10^{-31}	6.99×10^{-13}	1.79×10^{-12}	1.84×10^{-26}	1.79×10^{-12}
360	6.38×10^{-15}	4.55×10^{-23}	6.38×10^{-15}	1.14×10^{-12}	4.24×10^{-29}	1.14×10^{-12}	2.50×10^{-12}	2.43×10^{-24}	2.50×10^{-12}
368	7.29×10^{-15}	7.56×10^{-23}	7.29×10^{-15}	1.21×10^{-12}	9.07×10^{-29}	1.21×10^{-12}	2.62×10^{-12}	4.39×10^{-24}	2.62×10^{-12}

Table S7. Calculated CVT/SCT rate constants of H-abstraction and X-addition pathways of the Br + QCHO reaction system. (in $\text{cm}^3 \text{molecule}^{-1} \text{s}^{-1}$)

T(K)	Br + FCHO → products			Br + ClCHO → products			Br + BrCHO → products		
	Br- $k_{\text{abs-F}}$	Br- $k_{\text{add-F}}$	k_{total}	Br- $k_{\text{abs-Cl}}$	Br- $k_{\text{add-Cl}}$	k_{total}	Br- $k_{\text{abs-Br}}$	Br- $k_{\text{add-Br}}$	k_{total}
200	9.93×10^{-25}	2.41×10^{-42}	9.93×10^{-25}	4.20×10^{-17}	2.48×10^{-40}	4.20×10^{-17}	8.28×10^{-16}	8.69×10^{-76}	8.28×10^{-16}
244	1.46×10^{-22}	4.82×10^{-37}	1.46×10^{-22}	2.76×10^{-16}	2.03×10^{-35}	2.76×10^{-16}	2.85×10^{-15}	1.93×10^{-64}	2.85×10^{-15}
250	2.53×10^{-22}	1.83×10^{-36}	2.53×10^{-22}	3.43×10^{-16}	6.98×10^{-35}	3.43×10^{-16}	3.31×10^{-15}	3.35×10^{-63}	3.31×10^{-15}
260	6.02×10^{-22}	1.48×10^{-35}	6.02×10^{-22}	4.86×10^{-16}	4.84×10^{-34}	4.86×10^{-16}	4.21×10^{-15}	2.92×10^{-61}	4.21×10^{-15}
275	1.98×10^{-21}	2.58×10^{-34}	1.98×10^{-21}	7.87×10^{-16}	6.82×10^{-33}	7.87×10^{-16}	5.88×10^{-15}	1.29×10^{-58}	5.88×10^{-15}
280	2.86×10^{-21}	6.24×10^{-34}	2.86×10^{-21}	9.16×10^{-16}	1.55×10^{-32}	9.16×10^{-16}	6.55×10^{-15}	8.55×10^{-58}	6.55×10^{-15}
285	4.10×10^{-21}	1.47×10^{-33}	4.10×10^{-21}	1.06×10^{-15}	3.41×10^{-32}	1.06×10^{-15}	7.26×10^{-15}	5.29×10^{-57}	7.26×10^{-15}
295	8.11×10^{-21}	7.44×10^{-33}	8.11×10^{-21}	1.41×10^{-15}	1.53×10^{-31}	1.41×10^{-15}	8.88×10^{-15}	1.68×10^{-55}	8.88×10^{-15}
297	9.25×10^{-21}	1.02×10^{-32}	9.25×10^{-21}	1.49×10^{-15}	2.05×10^{-31}	1.49×10^{-15}	9.23×10^{-15}	3.27×10^{-55}	9.23×10^{-15}
298	9.87×10^{-21}	1.19×10^{-32}	9.87×10^{-21}	1.53×10^{-15}	2.36×10^{-31}	1.53×10^{-15}	9.41×10^{-15}	4.54×10^{-55}	9.41×10^{-15}
305	1.54×10^{-20}	3.40×10^{-32}	1.54×10^{-20}	1.85×10^{-15}	6.26×10^{-31}	1.85×10^{-15}	1.07×10^{-14}	4.27×10^{-54}	1.07×10^{-14}
360	2.91×10^{-19}	3.29×10^{-29}	2.91×10^{-19}	6.54×10^{-15}	3.63×10^{-28}	6.54×10^{-15}	2.67×10^{-14}	9.39×10^{-48}	2.67×10^{-14}
368	4.17×10^{-19}	7.56×10^{-29}	4.17×10^{-19}	7.67×10^{-15}	7.84×10^{-28}	7.67×10^{-15}	3.00×10^{-14}	5.48×10^{-47}	3.00×10^{-14}

Table S8. The modified Arrhenius formulas for $k = AT^B \exp(-C/T)$ for H-abstraction and X-addition pathways.

pathways	A	B	C
F-R _{abs-F}	4.58×10^{-16}	1.99	1104
F-R _{add-F}	5.80×10^{-32}	7.32	1932
F-R _{abs-Cl}	6.89×10^{-17}	2.16	716
F-R _{add-Cl}	2.59×10^{-32}	6.36	-1090
F-R _{abs-Br}	3.71×10^{-16}	1.91	374
F-R _{add-Br}	1.45×10^{-25}	5.27	3659
Cl-R _{abs-F}	1.80×10^{-41}	9.78	-1274
Cl-R _{add-F}	8.68×10^{-17}	1.29	7947
Cl-R _{abs-Cl}	5.39×10^{-18}	2.20	243
Cl-R _{add-Cl}	1.45×10^{-94}	26.66	2246
Cl-R _{abs-Br}	3.50×10^{-17}	1.91	31
Cl-R _{add-Br}	7.19×10^{-16}	1.11	9376
Br-R _{abs-F}	4.21×10^{-21}	3.02	4866
Br-R _{add-F}	1.25×10^{-17}	1.68	13165
Br-R _{abs-Cl}	1.53×10^{-23}	3.96	1228
Br-R _{add-Cl}	4.74×10^{-17}	1.42	12228
Br-R _{abs-Br}	5.41×10^{-24}	4.03	501
Br-R _{add-Br}	2.39×10^{-17}	1.61	18621

Table S9. The potential barrier heights (ΔE) and reaction enthalpies (ΔH_{298}^0) for elimination pathways of the F + QCHO reaction systems (Q = F, Cl and Br). (in kcal/mol, the energy of the corresponding IM is set to be zero as reference)

	ΔE	ΔH_{298}^0
F-R _{elm} -F1	10.80	-5.64
F-R _{elm} -F2	28.75	23.73
F-R _{elm} -F3	28.45	-24.87
F-R _{elm} -Cl1	11.06	-4.97
F-R _{elm} -Cl2	0.76	-15.17
F-R _{elm} -Cl3	25.54	-33.17
F-R _{elm} -Br1	7.64	-7.59
F-R _{elm} -Br2	-9.27	-31.49
F-R _{elm} -Br3	20.94	-42.44

Table S10. Calculated CVT/SCT rate constants of H-abstraction and X-addition pathways at different heights^a in the earth atmosphere. (in cm³ molecule⁻¹ s⁻¹)

h (km)	T (K)	F + FCHO → products		F + ClCHO → products		F + BrCHO → products	
		k _{abs}	k _{add}	k _{abs}	k _{add}	k _{abs}	k _{add}
0	298.15	9.28×10^{-13}	1.19×10^{-16}	1.40×10^{-12}	5.46×10^{-15}	5.65×10^{-12}	7.66×10^{-18}
0	288.19	7.63×10^{-13}	7.37×10^{-17}	1.19×10^{-12}	5.00×10^{-15}	5.07×10^{-12}	4.18×10^{-18}
2	275.21	5.81×10^{-13}	3.79×10^{-17}	9.60×10^{-13}	4.47×10^{-15}	4.37×10^{-12}	1.79×10^{-18}
4	262.23	4.33×10^{-13}	1.85×10^{-17}	7.60×10^{-13}	4.01×10^{-15}	3.72×10^{-12}	7.10×10^{-19}
6	249.25	3.14×10^{-13}	8.47×10^{-18}	5.90×10^{-13}	3.62×10^{-15}	3.12×10^{-12}	2.57×10^{-19}
8	236.27	2.21×10^{-13}	3.65×10^{-18}	4.48×10^{-13}	3.28×10^{-15}	2.59×10^{-12}	8.45×10^{-20}
10	223.29	1.51×10^{-13}	1.49×10^{-18}	3.33×10^{-13}	2.99×10^{-15}	2.11×10^{-12}	2.50×10^{-20}
12	216.69	1.22×10^{-13}	9.27×10^{-19}	2.83×10^{-13}	2.86×10^{-15}	1.88×10^{-12}	1.29×10^{-20}
h (km)	T (K)	Cl + FCHO → products		Cl + ClCHO → products		Cl + BrCHO → products	
		k _{abs}	k _{add}	k _{abs}	k _{add}	k _{abs}	k _{add}
0	298.15	2.11×10^{-15}	3.65×10^{-25}	6.53×10^{-13}	6.58×10^{-32}	1.71×10^{-12}	8.88×10^{-27}
0	288.19	1.75×10^{-15}	1.39×10^{-25}	5.89×10^{-13}	2.13×10^{-32}	1.60×10^{-12}	2.88×10^{-27}
2	275.21	1.37×10^{-15}	3.57×10^{-26}	5.12×10^{-13}	4.62×10^{-33}	1.46×10^{-12}	5.90×10^{-28}
4	262.23	1.07×10^{-15}	8.04×10^{-27}	4.40×10^{-13}	9.17×10^{-34}	1.32×10^{-12}	1.04×10^{-28}
6	249.25	8.39×10^{-16}	1.56×10^{-27}	3.75×10^{-13}	1.61×10^{-34}	1.19×10^{-12}	1.52×10^{-29}
8	236.27	6.59×10^{-16}	2.52×10^{-28}	3.16×10^{-13}	2.43×10^{-35}	1.07×10^{-12}	1.82×10^{-30}
10	223.29	5.21×10^{-16}	3.31×10^{-29}	2.63×10^{-13}	3.02×10^{-36}	9.50×10^{-13}	1.70×10^{-31}
12	216.69	4.63×10^{-16}	1.08×10^{-29}	2.38×10^{-13}	9.59×10^{-37}	8.94×10^{-13}	4.57×10^{-32}
h (km)	T (K)	Br + FCHO → products		Br + ClCHO → products		Br + BrCHO → products	
		k _{abs}	k _{add}	k _{abs}	k _{add}	k _{abs}	k _{add}
0	298.15	9.97×10^{-21}	1.21×10^{-32}	1.54×10^{-15}	2.41×10^{-31}	9.44×10^{-15}	4.77×10^{-55}
0	288.19	5.12×10^{-21}	2.49×10^{-33}	1.16×10^{-15}	5.57×10^{-32}	7.75×10^{-15}	1.64×10^{-56}
2	275.21	2.01×10^{-21}	2.67×10^{-34}	7.92×10^{-16}	7.06×10^{-33}	5.91×10^{-15}	1.40×10^{-58}
4	262.23	7.25×10^{-22}	2.31×10^{-35}	5.23×10^{-16}	7.31×10^{-34}	4.43×10^{-15}	7.55×10^{-61}
6	249.25	2.37×10^{-22}	1.55×10^{-36}	3.34×10^{-16}	6.00×10^{-35}	3.25×10^{-15}	2.37×10^{-63}
8	236.27	6.89×10^{-23}	7.81×10^{-38}	2.06×10^{-16}	3.76×10^{-36}	2.34×10^{-15}	3.95×10^{-66}
10	223.29	1.76×10^{-23}	2.79×10^{-39}	1.22×10^{-16}	1.71×10^{-37}	1.65×10^{-15}	3.15×10^{-69}
12	216.69	8.26×10^{-24}	4.40×10^{-40}	9.15×10^{-17}	3.09×10^{-38}	1.36×10^{-15}	6.06×10^{-71}

^a In the troposphere, the temperature drops about 6.49 K for every 1 km increase in altitude. Into the stratosphere (from 11 km height above the earth surface), the constant temperature is 216.69 K ([Wikipedia](http://en.wikipedia.org/wiki/Main_Page), http://en.wikipedia.org/wiki/Main_Page).

REFERENCES

- Bednarek, G., Breil, M., Hoffmann, A., Kohlmann, J. P., Mors, V., and Zellner, R.: Rate and mechanism of the atmospheric degradation of 1,1,1,2-tetrafluoroethane (HFC-134a), Ber. Bunsen. Phys. Chem., 100, 528-539, 1996.
- Behr, P., Goldbach, K., and Heydtmann, H.: The reaction of fluorine atoms with formyl fluoride and the CFO self-reaction at 293 K, Int. J. Chem. Kinet. , 25, 957-967, 1993.
- Behr, P., Kaupert, C., Shafranovski, E., and Heydtmann, H.: Temperature dependence of the gas-phase reactions F+CHFO, CFO+F, and CFO+CFO, Int J Chem Kinet, 30, 329-333, 1998.
- Catoire, V., Lesclaux, R., Schneider, W. F., and Wallington, T. J.: Kinetics and mechanisms of the self-reactions of CCl_3O_2 and CHCl_2O_2 radicals and their reactions with HO_2 , J. Phys. Chem. , 100, 14356-14371, 1996.
- Edney, E. O., and Driscoll, D. J.: Chlorine initiated photooxidation studies of hydrochlorofluorocarbons (HCFCs) and hydrofluorocarbons (HFCs): Results for HCFC-22 (CHClF_2); HFC-41 (CH_3F); HCFC-124 (CClFHC_3); HFC-125 (CF_3CHF_2); HFC-134a ($\text{CF}_3\text{CH}_2\text{F}$); HCFC-142b (CClF_2CH_3); and HFC-152a (CHF_2CH_3), Int. J. Chem. Kinet. , 24, 1067-1081, 1992.
- Francisco, J. S., and Zhao, Y.: The reaction of atomic fluorine with formyl fluoride: An experimental and theoretical study, J. Chem. Phys. , 93, 276-286, 1990.
- Groner, P., and Warren, R. D.: Approximate r(e) structures from experimental rotational constants and ab initio force fields, J. Mol. Struct. , 599, 323-335, 2001.
- Hasson, A. S., Moore, C. M., and Smith, I. W. M.: The fluorine atom initiated oxidation of CF_3CFH_2 (HFC-134a) studied by FTIR spectroscopy, Int. J. Chem. Kinet. , 30, 541-554, 1998.
- Huisman, P. A. G., Klebe, K. J., Mijlhoff, F. C., and Renes, G. H.: Molecular-structure of formyl fluoride in the gas-phase as determined from electron-diffraction and microwave data, J. Mol. Struct. , 57, 71-82, 1979.
- Ji, Y. M., Zhao, X. L., Liu, J. Y., Wang, Y., and Li, Z. S.: Theoretical dynamic studies on the reactions of $\text{CH}_3\text{C}(\text{O})\text{CH}_3\text{-nCl}_n$ (n=0-3) with the chlorine atom, J Comput Chem, 29, 809-819, 2008.
- Libuda, H. G., Zabel, F., Fink, E. H., and Becker, K. H.: Formyl chloride: UV absorption cross sections and rate constants for the reactions with Cl and OH, J. Phys. Chem. , 94, 5860-5865, 1990.
- Liu, Y. P., Lu, D. H., Gonzalezlafont, A., Truhlar, D. G., and Garrett, B. C.: Direct dynamics calculation of the kinetic isotope effect for an organic hydrogen-transfer reaction, including corner-cutting tunneling in 21 Dimensions, J. Am. Chem. Soc. , 115, 7806-7817, 1993.
- Meagher, R. J., McIntosh, M. E., Hurley, M. D., and Wallington, T. J.: A kinetic study of the reaction of chlorine and fluorine atoms with $\text{HC}(\text{O})\text{F}$ at 295+-2 K, Int J Chem Kinet, 29, 619-625, 1997.
- Nagai, K., Yamada, C., Endo, Y., and Hirota, E.: Infrared diode-laser spectroscopy of FCO- the NU-1 and NU-2 bands, J. Mol. Spectrosc. , 90, 249-272, 1981.
- NIST: <http://webbook.nist.gov/chemistry/>.
- Orlando, J. J.: Temperature dependence of the rate coefficients for the reaction of chlorine atoms with chloromethanes, Int. J. Chem. Kinet. , 31, 515-524, 1999.
- Pacey, P. D.: Changing Conceptions of Activation-Energy, J. Chem. Educ. , 58, 612-614, 1981.
- Sanhueza, E., and Heicklen, J.: Chlorine-atom sensitized oxidation of dichloromethane and chloromethane, J. Phys. Chem. , 79, 7-11, 1975.
- Szabo, A., and Ostlund, N. S.: Modern quantum chemistry, McGraw-Hill: New York, 1997.
- Truhlar, D. G., and Garrett, B. C.: Variational Transition-State Theory, Acc. Chem. Res. , 13, 440-448, 1980.
- Wallington, T. J., Hurley, M. D., Ball, J. C., and Kaiser, E. W.: Atmospheric chemistry of hydrofluorocarbon 134a: Fate of the alkoxy radical CF_3CFHO , Environ. Sci. Technol., 26, 1318-1324, 1992.
- Wallington, T. J., Hurley, M. D., and Schneider, W. F.: Atmospheric chemistry of CH_3Cl : Mechanistic study of the reaction of CH_2ClO_2 radicals with HO_2 , Chem. Phys. Lett. , 251, 164-173, 1996.
- Wikipedia, http://en.wikipedia.org/wiki/Main_Page.
- Wu, H. Y., Liu, J. Y., Li, Z. S., Huang, X. R., and Sun, C. C.: Theoretical study and rate constant calculation for the F+CHFO reaction, Chemical Physics Letters, 369, 504-512, 2003.